energies

MDPI

Article

Research on Intelligent Comprehensive Evaluation of Coal Seam Impact Risk Based on BP Neural Network Model

Kexue Zhang [1,2,3,4,5,6,*], Junao Zhu [1,3,*], Manchao He [2], Yaodong Jiang [2,4], Chun Zhu [7], Dong Li [1,3,6], Lei Kang [1,3], Jiandong Sun [1,3,6], Zhiheng Chen [1,3,6], Xiaoling Wang [1,3], Haijiang Yang [1,3], Yongwei Wu [1,3] and Xingcheng Yan [1,3]

1 Hebei Key Laboratory of Mine Intelligent Unmanned Mining Technology, North China Institute of Science and Technology, Beijing 101601, China; 201901377ld@ncist.edu.cn (D.L.); 201908522470kl@ncist.edu.cn (L.K.); 201801313sjd@ncist.edu.cn (J.S.); chengzhiheng21@ncist.edu.cn (Z.C.); back2019111@gmail.com (X.W.); yanghaijiang1105@gmail.com (H.Y.); wuyongweivyv@gmail.com (Y.W.); yanxingchen0044@gmail.com (X.Y.)
2 State Key Laboratory for Geomechanics and Deep Underground Engineering, China University of Mining and Technology (Beijing), Beijing 100083, China; hemanchaocumtb@163.com (M.H.); jiangyd@cumtb.edu.cn (Y.J.)
3 Institute of Intelligent Unmanned Mining, North China Institute of Science and Technology, Beijing 101601, China
4 State Key Laboratory of Coal Resources and Mine Safety, China University of Mining & Technology (Beijing), Beijing 100083, China
5 China Coal Research Institute, Beijing 100013, China
6 School of Mine Safety, North China Institute of Science and Technology, Beijing 101601, China
7 School of Earth Sciences and Engineering, Hohai University, Nanjing 210098, China; zhu.chun@hhu.edu.cn
* Correspondence: zhangkexue@ncist.edu.cn (K.Z.); zhujunao321@gmail.com (J.Z.); Tel.: +86-133-6603-0731 (K.Z.)

Abstract: Coal seam impact risk assessment is the premise of coal mine safety, which can reduce the occurrence of underground impact pressure accidents and directly affect the safety, coal production, economic and social benefits of coal mining enterprises. In order to evaluate the impact risk of coal seams more reasonably and comprehensively, and consider the weights of different influencing factors on the impact risk of coal seams, the neural network model is proposed to evaluate the impact risk of coal seams. Mining depth, impact tendency, geological structure and mining technology are selected as the influencing factors of coal seam impact risk. Each influencing factor contains different evaluation indices, a total of 18. The 18 evaluation indices and the impact risk level are normalized and quantified. The BP neural network model for evaluating coal seam impact risk level is established, and the impact risk of 2-1 coal seams in a mine in Inner Mongolia is comprehensively evaluated and analyzed in this study. The results show that the BP neural network model can represent coal seam impact risk level well. The application of the BP neural network model to evaluate coal seam impact risk level has the characteristics of high precision, fast calculation speed and less artificial calculation, which provides an efficient and convenient method for the evaluation of coal seam impact risk.

Keywords: coal seam; coal bump; impact risk; comprehensive evaluation; BP neural network; intelligent

check for updates

Citation: Zhang, K.; Zhu, J.; He, M.; Jiang, Y.; Zhu, C.; Li, D.; Kang, L.; Sun, J.; Chen, Z.; Wang, X.; et al. Research on Intelligent Comprehensive Evaluation of Coal Seam Impact Risk Based on BP Neural Network Model. *Energies* **2022**, *15*, 3292. https://doi.org/10.3390/en15093292

Academic Editors: Ingo Pecher and Athanasios Kolios

Received: 14 March 2022
Accepted: 27 April 2022
Published: 30 April 2022

Publisher's Note: MDPI stays neutral with regard to jurisdictional claims in published maps and institutional affiliations.

Copyright: © 2022 by the authors. Licensee MDPI, Basel, Switzerland. This article is an open access article distributed under the terms and conditions of the Creative Commons Attribution (CC BY) license (https://creativecommons.org/licenses/by/4.0/).

1. Introduction

In recent years, with increasing demand for coal, the mining depth of coal mines has deepened, accompanied by frequent underground impact pressure accidents. According to statistics, in the past 30 years, the number of coal bump mines in my country has rapidly increased from 32 in 1985 to 133 in 2020 [1]. Especially in the past two years, there have been five major underground impact pressure accidents: "Longyun 10.20", "Longjiabao 6.9", "Tangshan 8.2", "Shandong New Julong 2.22", and "Longyu Coal Mine" [2]. Underground impact pressure has become one of the most serious natural disasters affecting the safety of coal mines in my country [3]. Therefore, in recent years, in order to reduce the occurrence of underground impact pressure accidents, in addition to the development of intelligent coal

mines [4], the state has attached great importance to the safety of coal mine production and the impact of coal bump disasters in coal mine safety is becoming increasingly important. It is necessary to study and evaluate the impact risk of coal seams in mines.

At present, many domestic scholars are devoted to research of coal bump. Zhang Xiufeng et al. [5] applied multi-parameter joint monitoring and an early warning method to set the weight coefficient of coal bump factors, and realized classification monitoring and early warning of coal bump; Sun Litian et al. [6]. By analyzing field experimental data, the stress increment influence coefficient of each underground impact pressure influencing factor under the square is obtained, which provides a reference for multi-factor stress superimposed underground impact pressure evaluation; Zhang Ke et al. [7]. For the evaluation method of coal seam shock risk, a fuzzy comprehensive evaluation relationship matrix was established, and a fuzzy comprehensive evaluation model of coal seam shock risk was constructed, and its feasibility was verified through engineering examples; Jia Baoxin et al. [8]. Real-time monitoring is carried out in the field, and key monitoring is carried out to determine the coal bump area, by means of the mine pressure monitoring method and the drilling cutting method, so as to achieve the purpose of predicting coal bump. After analyzing a large number of micro-seismic events, Xie Jiahao [9] proposed a method of using micro-seismic means to monitor hidden faults in the working face; Wang Jiaxin et al. [10] established a PNN model for the evaluation of coal mine impact risk grades on the basis of R-type factor analysis, which provided a new method for coal seam impact risk assessment; Rong Hai et al. [11] applied the multi-factor pattern recognition method to predict the impact risk of steeply inclined extra-thick coal seams, and compared the prediction results of the comprehensive index method, which confirmed that the multi-factor pattern recognition method had better prediction results; Liu Xiaoyue et al. [12]. By improving the fruit fly optimization algorithm, it can be used to adjust the weights and thresholds of the BP network adaptively; Yin Zengde et al. [13] proposed a new method for local optimum and low accuracy in traditional coal bump prediction. The BP neural network algorithm, based on the chaotic optimization particle swarm, improves the accuracy of prediction; Yang Kai et al. [14] reduced the calculation process of the BP network by combining the principal component analysis method with the BP network; Lu Meining [15] et al. The influence factors of underground impact pressure are analyzed by gray correlation degree, and the BP network is predicted with a high correlation degree, and the prediction model put into practical application. In addition, there are other evaluation methods, such as the comprehensive index method [16], the possibility index method [17], the PSO-BP model [18], the AFOA-ELM model [19], and the new TOPSIS model [20].

The occurrence of underground impact pressure is a complex dynamic system, and the determination of the influence weight of each influencing factor on the risk of coal seam shock is a very complicated problem, so it is difficult to use a certain mathematical model to reflect the impact factors and coal seam shock functional relationship between risks. Since the neural network learns and trains the weights between the layers of the network through a large number of sample values, complex nonlinear problems are represented by the weights of the network [21]. At present, the common neural network prediction methods are artificial neural network (ANN), recurrent neural network (RNN) and convolutional neural network (CNN). ANN is commonly used to predict Tabular data, RNN is commonly used to predict Sequence data, and CNN is commonly used to predict Image data. Therefore, this paper applies BP neural network technology to evaluate coal seam impact risk. The evaluation index of coal seam shock risk is determined, the BP neural network model of coal seam shock risk is established, and the BP neural network is verified by engineering examples to calculate the coal seam shock risk level well.

2. Influence Factor Analysis of Coal Seam Underground Impact Pressure

Coal bump has a relatively complex mechanism, and its occurrence does not depend on one or several specific factors, but is mainly due to the interference of natural conditions and human factors [1]. It is necessary to fully consider the possibility of on-site data collection

and the effectiveness, pertinence, and accuracy of the influencing factors themselves to indicate the key influencing factors, and to select the four major influencing factors of mining depth, shock tendency, geological structure, and mining technology to impact ground pressure. Evaluation is then required.

2.1. Mining Depth

Under normal circumstances, the deeper the mining depth of the coal seam in the mine, the greater the in-situ stress on the coal body, and the higher the possibility of the risk of coal seam impact in the mine. Zhang Kexue et al. [22] used FLAC3D numerical simulation software to intuitively display the changes of in-situ stress at different depths, and qualitatively proved that mining depth affects the occurrence of coal seam impact risk in mines.

2.2. Impact Propensity

Impact tendency refers to the natural property of whether a coal rock mass is capable of underground impact pressure. The underground impact pressure tendency is an important basis for evaluating the risk of underground impact pressure in coal mines. The impact tendency is divided into coal seam impact tendency and roof and floor impact tendencies [23,24]. According to the relevant national standards for underground impact pressure in my country, and the rules for preventing and controlling underground impact pressure in coal mines, this paper divides the impact tendency index into the uniaxial compressive strength of coal, the uniaxial compressive strength of coal, the elastic energy index, dynamic failure time of coal [25], impact propensity of roof strata and impact propensity of floor strata. The uniaxial compressive strength of coal refers to the ratio of the failure load to the compressive area of the standard coal specimen under uniaxial compression [26]. The elastic energy index of coal refers to the ratio of the elastic deformation energy to the plastic deformation energy (loss change performance) of the coal specimen under uniaxial compression when force reaches a certain value (before failure) and unloading [27]. Under the same conditions, coal with higher impact tendency is more likely to have impact risk [28].

2.3. Geological Structure

Geological structure [29] has always been the key research object of coal mine safety production. Common types of geological structures include fault influence, fold structure, collapse column influence, and river scour zone influence. Yu Demian et al. [30] observed, through field observation, that when the mining direction of the working face is approximately perpendicular to the principal structural stress, underground impact pressure is likely to occur and strength is high. The intensity and frequency of pressure are greatly reduced.

2.4. Mining Technology

Mining technical conditions include the length of the working face, the width of the coal pillar in the section, the thickness of the bottom coal, the degree of pressure relief of the protective layer, the empty parameters of the working face, and the coal mining technology of the working face.

The protective layer pressure relief mining parameters include the pressure relief degree of the protective layer and the horizontal distance between the working face and the coal pillar left by the mining of the upper protective layer. The working face goaf parameters include the relationship between the working face and the adjacent goaf, and the working face mining parameters include working face length, section coal pillar width, and bottom coal thickness. Due to the wide distribution of coalfields in my country, and the complex geological conditions, the depth, thickness, type and other coal conditions of coal seams are all different, and the corresponding mining technologies are also very different. The traditional coal mining process greatly damages the stability of the coal seam,

and the danger of underground impact pressure is evident. Therefore, the coal mining process should be reasonably selected to improve production efficiency of the mine.

Figure 1 refers to 18 evaluation indexes of underground impact pressure risk in coal seams. Analyzing the influence of each impact index on the risk of coal seam impact, it can be seen that there is a nonlinear functional relationship between the risk of coal seam impact and each impact index. This functional relationship is difficult to give by conventional mathematical expressions. This paper adopts the BP neural network model. The operation process of BP neural network is divided into three parts: model establishment, training and application.

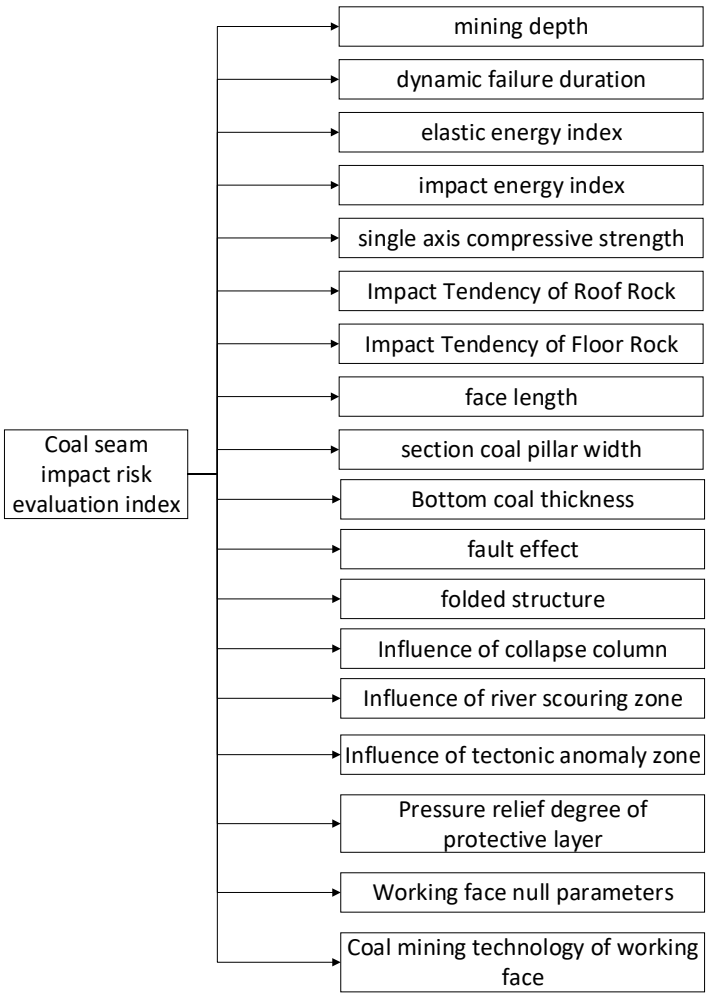

Figure 1. Evaluation Index of Coal Seam Impact Risk.

3. Establishment of BP Neural Network Model for Coal Seam Impact Risk

Figure 2 is the structure diagram of the BP neural network evaluation model. The BP algorithm is an effective method to calculate the partial derivative. Its basic principle is that the partial derivative of the error is calculated by using the results of the forward propagation and the final output. Then, the partial derivative and the front hidden layer are weighted and summed up, so that there is one layer of the back propagation, until the input layer (without calculating the input layer), and, finally, the weight, are updated, by using the partial derivative of each node. In the BP neural network evaluation model, the input and output layers are one layer, and the number of hidden layers needs to be determined. A large number of theoretical studies have shown that any continuous function in the closed interval can be approximated by a hidden layer of BP network. Therefore, this study uses the BP neural network evaluation model at the input layer, hidden layer and output layer.

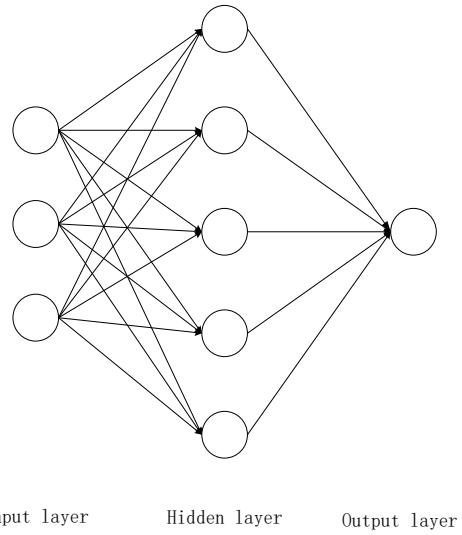

Figure 2. Structure diagram of BP neural network.

3.1. Determination of Input Layer and Output Layer Neurons

In the BP neural network, the number of neurons in the input layer and output layer is determined by the specific problem. The number of neurons in the input layer depends on the dimension of the data source taken. This paper uses the evaluation index of coal seam impact risk. The number of neurons in the output layer depends on the classification of the subject. By referring to relevant literature and relevant national standards of underground impact pressure in my country, the risk of coal seam underground impact pressure is divided into four categories: no impact, weak impact, medium impact and strong impact. That is, the model defines 18 input layer neurons, 1 output layer neuron.

In order to meet the calculation requirements of the BP neural network, it is necessary to quantify the indicators that affect the risk of coal seam impact. The quantitative representation method of the input layer is as follows:

(1) Mining depth (h): 0 is h $\leq$ 400 m, 1 is 400 m < h $\leq$ 600 m, 2 is 600 m < h $\leq$ 800 m, 3 is mining depth > 800 m;
(2) Dynamic destruction time (DT): 1 is DT > 500 ms, 2 is 50 ms < DT $\leq$ 500 ms, 3 is DT $\leq$ 50 ms;
(3) Elastic energy index (WET): 0 is WET < 2, 1 is 2 $\leq$ WET < 3.5, 2 is 3.5 $\leq$ WET < 5, 3 is WET $\geq$ 5;
(4) Impact energy index (KE): 1 is KE < 1.5, 2 is 1.5 $\leq$ KE < 5, 3 is KE $\geq$ 5;
(5) Uniaxial compressive strength (Rc): 0 is Rc $\leq$ 10 MPa, 1 is 10 MPa < Rc $\leq$ 14 MPa, 2 is 14 MPa <Rc $\leq$ 20 MPa, 3 is Rc $\geq$ 20 MPa;
(6) Impact tendency (UWQS) of roof rock stratum: 1 means no impact tendency UWQS $\leq$ 15 kJ, 2 means weak impact tendency 15 kJ < UWQS $\leq$ 120 kJ, 3 means strong impact tendency UWQS > 500 kJ;
(7) Impact tendency (UWQS) of floor rock formation: 1 means no impact tendency UWQS $\leq$ 15 kJ, 2 means weak impact tendency 15 kJ < UWQS $\leq$ 120 kJ, 3 means strong impact tendency UWQS > 500 kJ;
(8) Fault influence: 0 means no fault influence, 1 means the fault influence is small, 2 means the fault influence is large, and 3 means the fault influence is big;
(9) Fold structure: 0 means the fold structure is simple, 1 means the fold structure is general, 2 means the fold structure is more complicated, and 3 means the fold structure is complex;
(10) Influence of collapsed column: 0 means no impact of collapsed column, 1 means less impact of collapsed column, 2 means greater impact of collapsed column, 3 means greater impact of collapsed column;

(11) Impact of river scour zone: 0 means no river scour zone impact, 1 means river scour zone has less impact, 2 means river scour zone has greater impact, 3 means river scour zone has great influence;
(12) Working face length (L): 0 is L > 300 m, 1 is 150 m$\leq$ L < 300 m, 2 is 100 m $\leq$L < 150 m, 3 is L < 100 m;
(13) Section coal pillar width (d): 0 is d $\leq$ 3 m or d $\geq$ 50 m, 1 is 3 m < d $\leq$ 6 m, 2 is 6 m < d $\leq$ 10 m, 3 is 10 m < d < 50 m;
(14) Bottom coal thickness (td): 0 is td = 0 m, 1 is 0 m < td $\leq$ 1 m, 2 is 1 m < td $\leq$ 2 m, 3 is td > 2 m;
(15) The degree of pressure relief of the protective layer: 0 is good, 1 is good, 2 is medium, and 3 is very poor;
(16) Working face empty parameters: 0 is solid coal working face, 1 is empty on one side, 2 is empty on both sides, and 3 is empty on three sides;
(17) Coal mining process of working face: 0 is intelligent mining, 1 is fully mechanized mining, 2 is general mining, and 3 is blast mining;
(18) Influence of structural anomaly zone: 0 means no structural anomaly zone influence, 1 means that the structural anomaly zone has little influence, 2 means that the structural anomaly zone has a great influence, and 3 means that the structural anomaly zone has a great influence.

The quantification of the output layer is 0 for no shock risk, 1 for weak shock risk, 2 for medium shock risk, and 3 for strong shock risk.

3.2. The Number of Neurons in the Hidden Layer Is Determined

In the process of network design, it is very important to determine the number of neurons in the hidden layer. Too many neurons in the hidden layer will increase the amount of network computation and easily lead to overfitting problems; too few neurons will affect the network performance and fail to achieve the expected results [31]. The number of neurons in the hidden layer in the network is directly related to the complexity of the actual problem, the number of neurons in the input and output layers, and the setting of the expected error. This study uses Formula (1) to determine the number of neurons in the hidden layer [32].

$$\mathrm{h} = \sqrt{m+n} + a \tag{1}$$

In Formula (1) h represents the number of neurons in the hidden layer, m represents the number of neurons in the input layer, and n represents the number of neurons in the output layer, $a \in [1, 10]$. Substitute the number of neurons in the input and output layers into Formula (1), The range of the number of neurons in the hidden layer can be obtained as h $\in [5, 15]$. Comparing the prediction results of different numbers of neurons in the hidden layer, the calculation accuracy is high when the number of neurons in the hidden layer is 6. Therefore, this model establishes a BP neural network evaluation model with 6 neurons in the hidden layer. In summary, the 3-layer neural network model established by this model is $18 \times 6 \times 1$.

4. Model Training Process

Under the initial conditions, the connection weights and thresholds between the layers in the constructed BP neural network are arbitrary, which will produce large errors and cannot represent the danger of coal seam underground impact pressures well. The data is used as a training sample to adjust the intermediate value of the BP neural network. When the error between the calculated result and the actual output result of the sample is reduced to the set target value, the BP neural network is trained and can be used for risk assessment of coal seam impact.

4.1. Training Samples

Table 1 show the sample quantitative data of this experimental study.

Table 1. Training sample data of BP neural network [17,33–36].

Index \ Number	1	2	3	4	5	6	7	8	9	10	11	12	13	14	15	16	17
Mining depth	0	3	1	2	3	2	2	1	1	1	0	2	1	1	1	2	2
Dynamic damage time	0	1	2	3	3	3	3	1	3	3	3	3	2	2	2	3	1
Elasticity index	3	0	1	3	3	3	3	0	2	3	3	3	2	2	3	3	1
Impact energy index	1	1	3	3	3	3	3	1	2	3	3	3	3	3	3	3	1
Uniaxial compressive strength	3	2	2	2	3	2	3	1	2	3	3	2	3	2	3	3	1
Impact Tendency of Roof Rock	1	1	3	2	2	1	3	1	1	3	3	2	2	1	1	1	1
Impact Tendency of Floor Rock	1	1	1	1	1	2	1	1	1	1	1	2	1	1	1	1	1
Working face length	1	1	2	2	1	0	1	1	1	1	1	0	1	0	0	0	1
Section coal pillar width	2	3	3	3	1	3	3	3	3	3	3	3	3	1	1	3	2
Bottom coal thickness	0	0	0	0	0	0	0	0	0	0	0	0	0	0	0	0	0
fault effect	1	2	0	1	3	1	2	0	0	1	3	1	1	0	0	0	1
Fold structure	0	0	2	1	2	1	1	1	1	2	0	2	1	1	0	1	1
Influence of collapse column	0	0	0	0	0	0	0	0	0	0	0	0	0	0	0	0	0
Influence of river scouring zone	0	0	0	0	0	0	0	0	0	0	0	0	0	0	0	0	0
Influence of tectonic anomaly zone	0	0	1	2	3	0	3	0	0	3	3	0	2	1	1	1	0
Pressure relief degree of protective layer	3	0	1	2	3	1	3	0	3	3	3	0	1	0	0	0	0
Working face null parameters	3	2	0	0	2	0	0	2	0	0	0	0	0	0	0	0	1
Coal mining technology of working face	1	1	1	1	1	1	1	1	1	1	1	1	1	2	2	2	1
Impact risk grade	3	2	1	2	3	2	3	0	1	3	3	2	2	1	1	2	0

Index \ Number	18	19	20	21	22	23	24	25	26	27	28	29	30	31	32	33	34
Mining depth	1	2	2	2	2	0	1	2	3	3	0	1	2	3	0	1	2
Dynamic damage time	1	3	2	3	3	2	2	2	2	1	1	1	1	1	1	1	1
Elasticity index	1	3	3	3	3	3	3	3	3	0	3	3	3	3	1	1	1
Impact energy index	1	3	3	3	3	3	3	3	3	1	2	2	2	2	3	3	3
Uniaxial compressive strength	1	2	3	3	3	3	3	3	3	2	2	2	2	2	3	3	3
Impact Tendency of Roof Rock	1	2	2	1	1	1	2	2	2	1	2	2	2	2	2	2	2
Impact Tendency of Floor Rock	1	2	2	1	1	1	2	2	2	1	2	2	2	2	2	2	2
Working face length	1	1	0	2	2	1	1	1	1	1	1	1	1	1	1	1	1
Section coal pillar width	2	3	3	1	2	3	3	3	3	3	3	3	3	3	3	3	3
Bottom coal thickness	0	0	0	0	0	0	0	0	0	0	2	1	1	2	0	0	0
fault effect	1	1	1	2	2	3	3	3	3	2	1	1	1	1	1	1	1
Fold structure	2	2	1	1	1	1	1	1	1	0	1	1	1	1	1	1	1
Influence of collapse column	0	0	0	0	0	0	0	0	0	0	0	0	0	0	0	0	0
Influence of river scouring zone	0	0	0	0	0	0	0	0	0	0	0	0	0	0	0	0	0
Influence of tectonic anomaly zone	2	0	0	3	3	1	1	1	1	0	1	1	1	1	1	1	1
Pressure relief degree of protective layer	0	0	0	0	0	0	0	0	0	0	0	0	0	0	0	0	0
Working face null parameters	1	0	1	1	0	1	1	1	1	2	1	1	1	1	1	1	1
Coal mining technology of working face	1	1	1	1	3	1	1	1	1	1	1	1	1	1	1	1	1
Impact risk grade	0	2	2	3	3	1	1	1	2	2	1	1	1	2	1	1	1

Table 1. *Cont.*

Index \ Number	35	36	37	38	39	40	41
Mining depth	3	2	3	3	3	3	3
Dynamic damage time	1	3	1	3	1	1	1
Elasticity index	1	3	1	3	1	1	2
Impact energy index	3	3	1	3	1	1	2
Uniaxial compressive strength	3	3	3	3	1	2	1
Impact Tendency of Roof Rock	2	2	3	3	2	2	2
Impact Tendency of Floor Rock	2	2	2	3	1	2	2
Working face length	1	0	1	0	0	0	0
Section coal pillar width	3	0	0	0	0	0	0
Bottom coal thickness	0	0	0	1	0	0	0
fault effect	1	1	3	3	2	2	3
Fold structure	1	1	1	1	1	1	1
Influence of collapse column	0	0	0	0	0	0	0
Influence of river scouring zone	0	0	0	0	0	0	0
Influence of tectonic anomaly zone	1	1	2	3	3	3	2
Pressure relief degree of protective layer	0	0	0	0	0	0	0
Working face null parameters	1	0	3	3	3	3	3
Coal mining technology of working face	1	1	1	1	1	1	0
Impact risk grade	2	2	3	3	3	3	3

4.2. Training Process

The training process of this model is divided into two parts: the forward propagation of the input signal and the back propagation of the error signal. There are 41 groups of learning samples, and the sample value of the coal seam underground impact pressure risk evaluation index is $X^k = \{x_1{}^k, x_2{}^k, \ldots, x_i{}^k, \ldots, x_{41}{}^k\}$ (k = 1, 2, . . . , 41). The sample value of the calculation result of the impact risk in the output coal seam is Y^k (k = 1, 2, . . . , 41). Neural network training is performed on these 41 sets of sample data, and each set of samples is forwarded first.

The forward propagation process of the BP neural network is that when the input layer neurons input 18 coal seam coal bump risk evaluation indicators x_i (i = 1, 2, . . . , 18), the input value is transmitted to the output layer through the hidden layer. Calculation results of coal seam underground impact pressure hazard risk: the connection weight components w_{ji}^l (i = 1, 2, . . . , 18; j = 1, 2, . . . , 5) between each layer are weighted and summed (where j is the hidden layer neuron), and then combined with the hidden layer neuron The threshold b_j^l is added. The activation function used by the neurons in the hidden layer of this model is tansig type. Its mathematical expression is

$$f(z) = \frac{2}{1 + e^{-2z}} - 1 \tag{2}$$

In Formula (2) z represents a variable. From this, the output value of each layer can be obtained as

$$a_j^l = f\left(\sum_{k=1}^{18} w_{ji}^l a_k^{l-1} + b_j^l\right) \tag{3}$$

In the Formula: a_j^l represents the output result of the j-th neuron in the l-th layer; a_k^{l-1} represents the input value of the k-th neuron in the $l-1$-th layer; w_j^l represents the connection weight component between the l-th layer and the $l-1$-th layer.

Figure 3 shows the neural network propagation process. From Figure 3, the input value can be obtained by referring to Formula (3) to obtain the parameters of each neuron

in the hidden layer, and then the parameters of the neurons in the hidden layer are used as input, and the output is obtained by referring to Formula (3) layer value again.

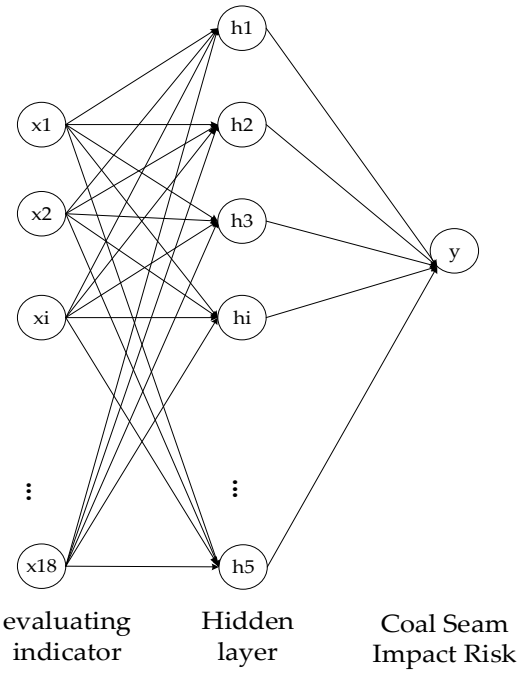

Figure 3. Propagation flow of BP neural network.

In order to avoid the output range being too small, due to the selection of tansig-type neurons, the output layer neurons use pureline-type linear functions. The mathematical expression of the calculation error of the objective function is:

$$E = \frac{1}{2}\sum_{k=1}^{K}(y^k - y^{k'})^2 \tag{4}$$

In the Formula (4): E represents the error; y^k represents the risk level of coal seam impact risk; $y^{k'}$ represents the output value of the network forward calculation.

If the error between the output result of the BP neural network and the risk level of coal seam impact is large, the error will be reversely transmitted to the input layer through the hidden layer, and the weights and thresholds between the layers will be adjusted according to the error to make them better reflect the actual risk of coal seam shock. The BP neural network achieves the purpose of learning through the gradient descent algorithm. The specific expression of the reverse adjustment weight from the output layer to the hidden layer is as follows:

$$\Delta w_j^2 = -\eta\frac{\partial E}{\partial w_j^2} = \eta \times (\mathrm{y} - \mathrm{y}') \times f'(\sum_{j=1}^{6} a_j w_j^2 + b^2) \times a_j \tag{5}$$

$$\Delta b^2 = -\eta\frac{\partial E}{\partial b^2} = \eta \times (\mathrm{y} - \mathrm{y}') \times f'(\sum_{j=1}^{6} a_j w_j^2 + b^2) \tag{6}$$

The specific expression of the reverse adjustment weight from the hidden layer to the output layer is:

$$\Delta w_{ji}^l = -\eta\frac{\partial E}{\partial w_{ji}^l} = \eta \times (\mathrm{y} - \mathrm{y}') \times f'(\sum_{j=1}^{6} a_j w_j^2 + b^2) \times w_j^2 \times f'(\sum_{k=1}^{18} x_k w_{ji}^l + b_j^l) x_k \tag{7}$$

$$\Delta b_j^l = -\eta \frac{\partial E}{\partial b_j^l} = \eta \times (\mathrm{y} - \mathrm{y}') \times f'(\sum_{j=1}^{6} a_j w_j^2 + b^2) \times w_j^2 \times f'(\sum_{k=1}^{18} x_k w_{ji}^l + b_j^l) \quad (8)$$

In the Formulas (5)–(8): η represents the learning step size; Δw_j^2, Δb^2, Δw_{ji}^l, Δb_j^l represents the forward adjustment amount.

Figure 4 shows the iterative process of training error. After adjusting the connection weights and thresholds between the input and output layers of the neurons in the hidden layer, Formulas (2) and (3) are called again for calculation. Then the error between the result calculated by the BP neural network and the coal seam impact risk level sample is calculated by Equation (4). If the error is too high, the connection weight and threshold are further adjusted according to Equations (5)–(8). The neural network is trained by repeated learning until the error reaches a given accuracy. The root mean square error of the model is 0.0032, and the average absolute error is 0.0016. Figure 5 is the regression curve. Figure 6 shows the network training process. From Figure 6, it can be seen that the network can calculate the coal seam impact risk level very well.

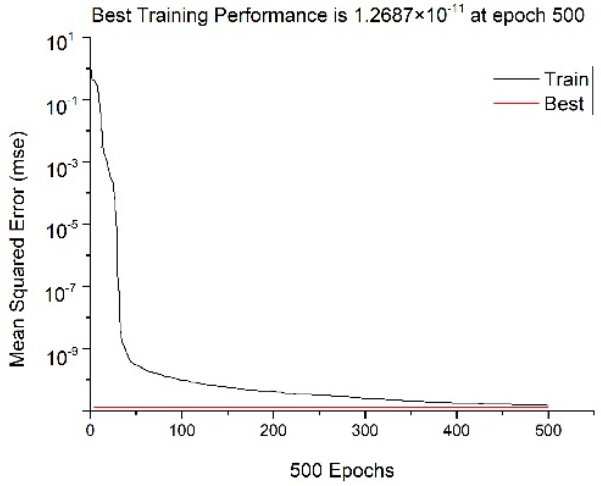

Figure 4. Iterative process of training error.

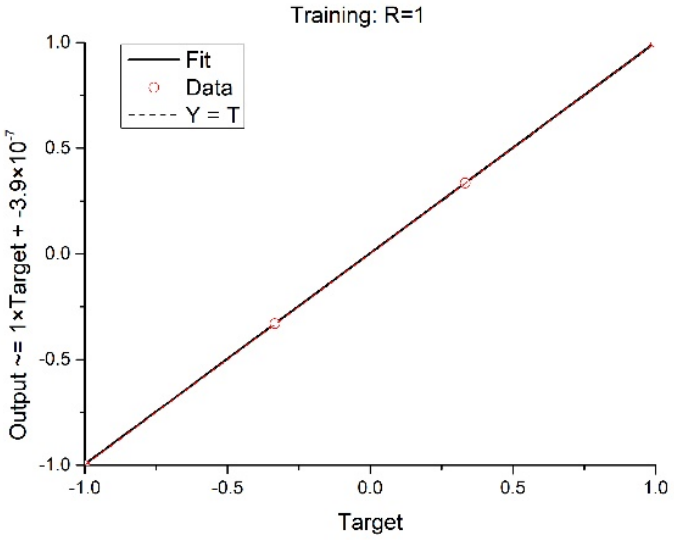

Figure 5. Regression analytical curve.

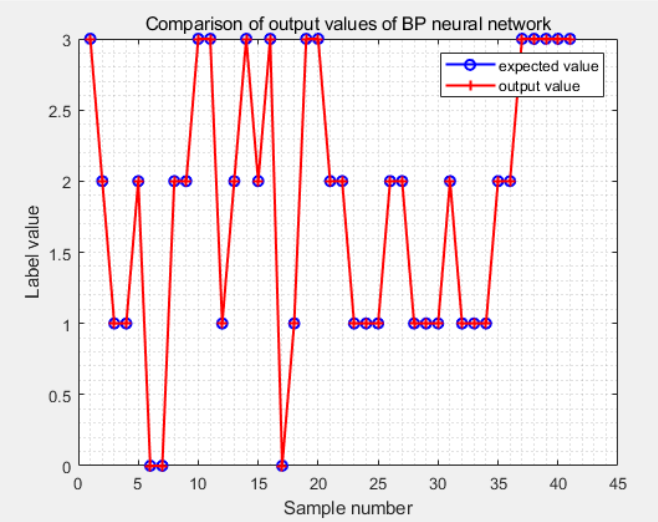

Figure 6. Network training performance analysis chart.

5. Project Example Application

Taking a mine in Inner Mongolia as an example, the coal seam impact risk of the 2-1 coal seam is evaluated to verify whether the constructed model can be used for mine coal seam impact risk assessment. It is known that the mining depth of the coal seam is 626.17 m~647.91 m, the average mining depth is 637 m, the average dynamic failure time is 45.6 ms, the average elastic energy index is 20.76, the average impact energy index is 10.03, and the average uniaxial compressive strength is 28.52 Mpa. The bending energy indices of the rock formation and the floor are 43.37 kJ and 69.51 kJ, respectively. The overall structural form of the minefield where the coal seam is located is a monoclinic structure inclined to the northwest, and a second-order undulating monoclinic structure is developed, and the formation dip angle is less than 2°. Among these, there are 4 folds (2 anticlines, 2 synclines), 6 faults (4 normal faults, 2 reverse faults), no river scour belts and collapse columns, and the minefield geological structure is simple.

Figure 7 shows the calculated value and error diagram of the impact risk level of the coal seam through the comprehensive index method [37]. Table 2 shows the values of each evaluation index after quantification. It can be seen from Figure 4 that the calculation results of the neural network are in line with the actual results. The neural network can represent the relationship between the input value and the output value well, and can evaluate the impact risk level of the coal seam well.

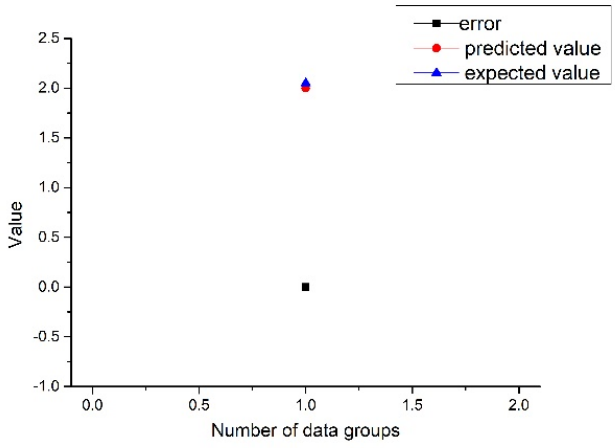

Figure 7. Data comparison chart.

Table 2. 2-1 Quantitative value of coal bed input layer.

Mining Depth	2
Dynamic damage time	3
Elasticity index	3
Impact energy index	3
Uniaxial compressive strength	3
Impact Tendency of Roof Rock	2
Impact Tendency of Floor Rock	2
Working face length	0
Section coal pillar width	3
Bottom coal thickness	0
fault effect	1
Fold structure	1
Influence of collapse column	0
Influence of river scouring zone	0
Influence of tectonic anomaly zone	0
Pressure relief degree of protective layer	0
Working face null parameters	0
Coal mining technology of working face	1
Impact risk grade	2

6. Conclusions

(1) It is determined that the influencing factors of coal seam shock risk are mining depth, shock tendency, geological structure and mining technology, and 18 indicators among the 4 major influencing factors were selected to establish a comprehensive evaluation model of coal seam shock risk BP neural network.
(2) It has been proved, by engineering examples, that the trained network model can evaluate the risk level of coal seam impact well, and the use of the BP neural network model can greatly reduce the amount of human calculation, and propose a new method for the study of coal seam impact risk evaluation in mines.
(3) It was found that the BP neural network method has good adaptability and accuracy in solving nonlinear problems, such as coal seam impact risk.

Author Contributions: Conceptualization, K.Z.; methodology, M.H.; software, J.Z. and Y.W.; validation, D.L., J.S. and Z.C.; formal analysis, C.Z., X.W., L.K. and. H.Y.; investigation, J.Z.; resources, K.Z.; data curation, J.Z., X.W., L.K. and X.Y.; writing—original draft preparation, J.Z.; writing—review and editing, J.Z. and L.K.; supervision, Y.J. and M.H.; project administration, J.Z.; funding acquisition, K.Z. All authors have read and agreed to the published version of the manuscript.

Funding: This research was funded by the State Key Laboratory of Deep Geomechanics and Underground Engineering (Beijing) Open Fund Project (SKLGDUEK1822, SKLGDUEK2133) the National Natural Science Foundation of China (51804160); Funded Projects for Fundamental Scientific Research Funds of Central Universities (3142019009); and Projects Supported by the Natural Science Foundation of Hebei Province (E2019508209).

Institutional Review Board Statement: Not applicable.

Informed Consent Statement: Not applicable.

Data Availability Statement: The data used to support the findings of this study are available from the corresponding author upon request.

Conflicts of Interest: The authors declare that there is no conflict of interest regarding the publication of this paper.

References

1. Qi, Q.X.; Zhao, S.K.; Li, H.T.; Qing, K. Several key problems of coal bump prevention and control in China's coal mines. *Saf. Coal Mines* **2020**, *51*, 135–143+151.
2. Jiang, Y.D.; Pan, Y.S.; Jiang, F.X.; Dou, L.M.; Ju, Y. Coal bump mechanism and prevention in coal mining in China. *J. China Coal Soc.* **2014**, *39*, 205–213.
3. Qi, Q.X.; Li, Y.Z.; Zhao, S.K.; Zhang, N.B.; Zheng, W.J.; Li, H.T.; Li, H.Y. Seventy years development of coal mine coal bump in China: Establishment and consideration of theory and technology system. *Coal Sci. Technol.* **2014**, *39*, 205–213.
4. Zhang, K.X.; Kang, L.; Chen, X.X.; He, M.C.; Zhu, C.; Li, D. A Review of Intelligent Unmanned Mining Current Situation and Development Trend. *Energies* **2022**, *15*, 513. [CrossRef]
5. Zhang, X.F.; Qun, X.C.; Wei, Q.D. Development and application of multi-dimension multi-parameter monitoring and early warning platform of coal bump. *J. Min. Strat. Control. Eng.* **2021**, *3*, 69–78.
6. Sun, L.T.; Kong, H.; Zhang, L.M.; Tian, G.Q.; Li, D.Y. Analysis of stress increment in multi-factor stress superposition underground impact pressure risk assessment. *Coal Eng.* **2020**, *52*, 94–98.
7. Zhang, K.X.; Kang, L.; He, M.C.; Liu, J.H.; Chen, Z.H.; Sun, J.D.; Li, D.; Zhao, Q.F.; Yin, S.F.; Shang, G.F.; et al. Research on multi-level comprehensive evaluation of coal seam coal bump risk in underground mine. *Coal Sci. Technol.* **2020**, *48*, 82–89.
8. Jia, B.X.; Chen, H.; Pan, Y.S.; Cheng, Y. Underground impact pressure prediction technology of multi-parameters synthetic index. *J. Disaster Prev. Mitig. Eng.* **2019**, *39*, 330–337.
9. Xie, J.H. Prediction of hidden faults in working face based on time-frequency-energy characteristic analysis of microseismical events. *Coal Eng.* **2020**, *52*, 114–119.
10. Wang, J.X.; Zhou, Z.H.; Li, K.G.; Wang, H.Q.; Fu, Z.G. Evaluation model for the risk grade of underground impact pressure based on the R-type factor analysis and a probabilistic neural network. *J. Vib. Shock.* **2019**, *38*, 192–203.
11. Rong, H.; Zhang, H.W.; Chen, J.Q.; Zhao, X.Z.; Sun, B.C. Coal bump-risk prediction in steep-inclined and extremely thick coal seams based on the multi-factor pattern recognition method. *J. Min. Saf. Eng.* **2018**, *35*, 125–132.
12. Liu, X.Y.; Li, P.Y. Prediction of coal bump based on improved FOA-BP neural network. *Min. Saf. Environ. Prot.* **2018**, *45*, 55–60.
13. Ying, Z.D.; Wang, L.H.; Liu, Y.N. Prediction of coal bump based on chaos particle swarm optimization BP neural network. *Coal Technol.* **2016**, *35*, 89–91.
14. Yang, K.; Chen, J.H. Research of underground impact pressure prediction based on combination of principal component analysis and neural network. *J. Guangxi Univ.* **2012**, *37*, 997–1003.
15. Lu, M.N.; Wang, C.; Sheng, W.Q.; Zhang, Y. Prediction of coal bump based on grey theory and neural network. *Coal Technol.* **2011**, *30*, 117–118.
16. Qu, K.D.; Ma, W.Q.; Liu, F.; Wang, T.X.; He, Y. The correction index of the mined-out area width in the comprehensive index method of rock pressure. *Coal Technol.* **2016**, *35*, 93–95.
17. Zou, L.Y. Underground impact pressure risk prediction in island working face based on multi-factor analysis. *Coal Eng.* **2019**, *51*, 96–100.
18. Song, J.; Wang, J.; Liu, S.; Bi, Y.F.; Wang, C. Prediction of underground impact pressure by electromagnetic radiation method based on improved PSO-BP model. *Saf. Coal Mines* **2019**, *50*, 205–208.
19. Wen, T.; Li, Y.Z. Risk prediction model of underground impact pressure based on reprocessing for AFOA-ELM. *China Saf. Sci. J.* **2019**, *29*, 29–34.
20. Zhang, Q.H.; Yao, Y.H.; Zhao, E.B. Underground impact pressure hazard prediction based on a new TOPSIS model. *Saf. Coal Mines* **2018**, *49*, 173–176.
21. Wang, Y.H.; Liu, L.L.; Fu, H.; Xu, Y.S. Study on predicted method of mine pressure bump based on improved BP neural network. *Coal Sci. Technol.* **2017**, *45*, 36–40.
22. Zhang, K.X. *Mechanism Study of Coal Bump under Tectonic and Ultra-Thick Conglomerate Coupling Conditions in Mining Roadway*; China University of Mining & Technology: Beijing, China, 2015.
23. Wang, Q.; He, M.C.; Li, S.C.; Jiang, Z.H.; Wang, Y.; Qin, Q.; Jiang, B. Comparative study of model tests on automatically formed roadway and gob-side entry driving in deep coal mines. *Int. J. Min. Sci. Technol.* **2021**, *31*, 591–601. [CrossRef]
24. Du, W.S.; Zhang, K.X.; Sun, H. Mechanical properties and energy development characteristics of impact-prone coal specimens under uniaxial cyclic loading. *AIP Adv.* **2019**, *9*, 115114. [CrossRef]
25. Wang, Q.; Xu, S.; He, M.C.; Jiang, B.; Wei, H.Y.; Wang, Y. Dynamic mechanical characteristics and application of constant resistance energy-absorbing supporting material. *Int. J. Min. Sci. Technol.* **2022**. [CrossRef]
26. Wu, Z.J.; Wang, Z.Y.; Fan, L.F.; Weng, L.; Liu, Q.S. Micro-failure process and failure mechanism of brittle rock under uniaxial compression using continuous real-time wave velocity measurement. *J. Cent. South Univ.* **2021**, *28*, 556–571. [CrossRef]
27. Su, Y.Q.; Gong, F.Q.; Luo, S.; Liu, Z.X. Experimental study on energy storage and dissipation characteristics of granite under two-dimensional compression with constant confining pressure. *J. Cent. South Univ.* **2021**, *28*, 848–865. [CrossRef]
28. Wang, Y.; Yang, H.N.; Han, J.Q.; Zhu, C. Effect of rock bridge length on fracture and damage modelling in granite containing hole and fissures under cyclic uniaxial increasing-amplitude decreasing-frequency (CUIADF) loads. *Int. J. Fatigue* **2022**, *158*, 106741. [CrossRef]
29. Zhu, C.; Karakus, M.; He, M.C.; Meng, Q.X.; Shang, J.L.; Wang, Y.; Yin, Q. Volumetric deformation and damage evolution of Tibet interbedded skarn under multistage constant-amplitude-cyclic loading. *Int. J. Rock Mech. Min. Sci.* **2022**, *152*, 105066. [CrossRef]

30. Yu, D.M.; Sun, B.Z. Analysis of geological structural stress and the cause mechanism of underground impact pressure in Taozhuang Mine. *J. China Coal Soc.* **1993**, *3*, 77–84.
31. Roshani, M.; Phan, G.; Faraj, R.H.; Phan, N.H.; Roshani, G.H.; Nazemi, B.; Corniani, E.; Nazemi, E. Proposing a gamma radiation based intelligent system for simultaneous analyzing and detecting type and amount of petroleum by-products. *Nucl. Eng. Technol.* **2021**, *53*, 1277–1283. [CrossRef]
32. Sattari, M.A.; Gholam, H.R.; Robert, H.; Ehsan, N. Applicability of time-domain feature extraction methods and artificial intelligence in two-phase flow meters based on gamma-ray absorption technique. *Measurement* **2021**, *168*, 108474. [CrossRef]
33. Zhu, F.; Zhang, H.W. "AHP +entropy weight method" based CW-TOPSIS model for predicting coal bump. *China Saf. Sci. J.* **2017**, *27*, 128–133.
34. Yan, H. *Research on Underground Impact Pressure Prediction Based on the Combination of Genetic Algorithm and Artificial Neural Network*; Chongqing University: Chongqing, China, 2002.
35. Shao, J.S. *Prediction Method of Dangerous Degree of Coal Resources Mining in Dynamic Disasters*; Shandong University of Science and Technology: Qingdao, China, 2011.
36. Zhou, X.W.; Yang, Y.W.; Yang, Y.K. Strata pressure behaviour degree based on comprehensive index method and BP neural network model. *Shanxi Coal* **2020**, *40*, 5–9.
37. Cheng, H.; Xia, C.P.; Duan, Y.Z.; Lin, C.H.; Rui, H.B.; Gao, Q. Research on Performance Evaluation of Scientific and Technological Achievements Transformation in High-level Science and Engineering Universities Based on Overall Correlation Coefficient Method and Comprehensive Index Method. *Sci. Technol. Manag. Res.* **2021**, *41*, 65–71.